Optics Letters

Recovery of wave-mixing conversion efficiency in weakly scattering nonlinear crystals

Zhuo Wang,[1,2] Yanqi Qiao,[1,2] Shuo Yan,[1,2] Haoying Wu,[1,2] Yuanlin Zheng,[1,2] and Xianfeng Chen[1,2,*]

[1]State Key Laboratory of Advanced Optical Communication Systems and Networks, School of Physics and Astronomy, Shanghai Jiao Tong University, Shanghai 200240, China
[2]Key Laboratory for Laser plasma (Ministry of Education), Collaborative Innovation Center of IFSA (CICIFSA), Shanghai Jiao Tong University, Shanghai 200240, China
*Corresponding author: xfchen@sjtu.edu.cn

Received 10 April 2018; accepted 3 July 2018; posted 10 July 2018 (Doc. ID 328120); published 31 July 2018

Nonlinear optical wave mixing is a widely used method to produce light with new frequencies that has a significant impact on laser technology and optical imaging. The most important figure of merit in wave-mixing processes, i.e., high conversion efficiency, is always required in laser applications. We demonstrate a method to recover high conversion efficiency of second harmonic generation in a $BaMgF_4$ single crystal with weakly scattering defects via feedback-based wavefront shaping under birefringent phase-matching condition. By optimizing the fundamental wavefront, a typical second harmonic output with an enhancement factor of 1.14 and a corresponding recovery efficiency of 86.3% is displayed. This investigation may modify the wide understanding of scattering in crystals and provide an avenue to recover the nonlinear optical conversion efficiency in crystals with various defects without special fabrications. © 2018 Optical Society of America

OCIS codes: (190.0190) Nonlinear optics; (290.5850) Scattering, particles; (190.4400) Nonlinear optics, materials; (190.4223) Nonlinear wave mixing.

https://doi.org/10.1364/OL.43.003734

For the past decades, three- or four-wave mixing in nonlinear materials is a convenient way to produce lasers with new frequencies from traditional lasers [1–3]. In nonlinear optical processes, high conversion efficiency is a key point for practical laser applications. High fundamental intensity [4], high nonlinear coefficient of the crystal, long interaction length [5], and phase-matching (PM) [6–9] are very important conditions to improve the conversion efficiency. Among these, PM is always thought to be the most vital part. To realize PM condition, optical dispersion that leads to phase mismatching of the interacting waves should be overcome, and various methods have been studied including birefringent phase matching (BPM) [6], quasi-phase matching (QPM) [10], Cherenkov-type phase matching [11,12], and random quasi-phase matching (RQPM) [13,14]. BPM is the most widely used PM method for its convenient realization and higher conversion efficiency.

Scattering, which used to be thought harmful in light propagation, has been drawing much attention in the past several years thanks to the application of feedback-based wavefront shaping in complex imaging [15], enhanced optical processes [16], and focusing through strongly scattering materials [17]. In these cases, the incident light is diffused by the turbid media. As we know, scattering defects in a single crystal decrease its transparency and cause optical loss. In nonlinear optical processes, scattering decreases the conversion efficiency as well. Unfortunately, scattering cannot be avoided completely during crystal growth in most circumstances [18,19]. In this Letter, we experimentally demonstrate the recovery of second harmonic (SH) output in a $BaMgF_4$ (BMF) single crystal with scattering defects via feedback-based wavefront shaping under BPM condition.

The concept of recovering SH via feedback-based wavefront shaping is presented in Fig. 1. In contrast to strongly scattering

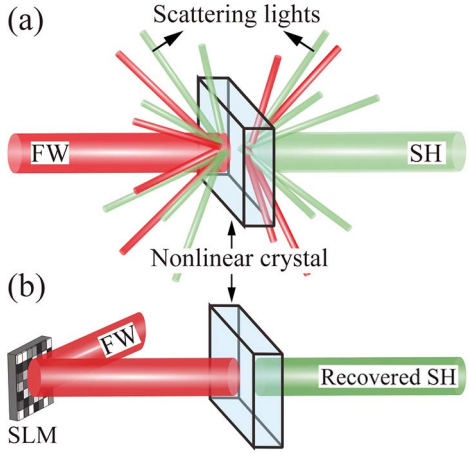

Fig. 1. Concept of recovering the SH conversion efficiency in weakly scattering crystals with scattering defects via feedback-based wavefront shaping. (a) Without wavefront shaping, some of the fundamental and generated SH beams would be disturbed because of scattering. (b) With proper phase masks added on the SLM, the intensity of the modulated BPM SH signal can be promoted through coherent superposition.

media—for example, powders—the nonlinear crystal with scattering defects can be regarded as a weakly scattering medium, which satisfies the relation of $k \cdot L \gg 1$, where k is the wave vector of the fundamental wave (FW) and L is the scattering free path. Considering the complicated process of scattering and SH generation (SHG), it is difficult to describe it as one simple theory, such as Huygens–Fresnel principle or nonlinear coupled-mode theory [20]. The whole SH process mixed with scattering can be regarded as two separate parts for simplicity. Some of the FW propagating through the crystal is not influenced by the scattering defects, and it experiences the ordinary SH process. The resting fundamental beam and generated SH beam affected by the scattering defects are totally disturbed, and they obey the theory proposed by Vellekoop and Mosk [21]. As a result, the transmitted field of each position i at the detected location, E_i^{out}, is a linear combination of the fields coming from the ordinary SH process and the modulated spatial light modulator (SLM). Thus, the total SH output field $\sum_i E_i^{\text{out}}$ at the detected location can be written as

$$\sum_i E_i^{\text{out}} = \sum_i \left(E_{oi} + \sum_{n=1}^{N} t_{ni} e^{j\phi_n} E_{ni} \right), \tag{1}$$

where E_{0i} represents the field of the SH beam, which meets the nonscattering situation, E_{ni} represents the field of scattering SH beam, and $t_{ni}e^{j\phi_n}$ is the coefficient of nth segment on the SLM with ϕ_n being the phase component. N is the total segments of the SLM.

Without SLM modulation, the SH emergent wavefront is distorted by scattering defects, as shown in Fig. 1(a), and the conversion efficiency of the SH is lower than that under the ideal situation. By shaping the incident light, the overall emergent SH field at the detected location is modulated and can lead to a constructive interference of the SH output. That is to say, the intensity of the modulated BPM SH signal can be promoted through coherent superposition by choosing proper phase masks of the SLM [Fig. 1(b)]. To realize that, a searching algorithm is employed to make sure the SH conversion efficiency is enhanced.

The schematic diagram of the experimental setup is illustrated in Fig. 2(a). The FW was a Q-switched nanosecond laser with pulse duration of 10 ns and a repetition rate of 500 Hz at 1064 nm wavelength. A half-wave plate and a Glan–Taylor polarizer were used to control the input power and polarization simultaneously. The FW was spatially expanded by the combination of Lenses 1 and 2 to cover as many as the segments of the SLM. The resolution of the SLM is 512 × 512 pixels, and the size of each pixel is 19.5 μm × 19.5 μm. The shaped FW was then spatially shrunk and irradiated into the nonlinear sample through a 4f optical imaging system (Lenses 3 and 4) to realize frequency doubling. At last, the SH light was imaged on a charge-coupled device (CCD) after passing through an infrared cutoff filter. The CCD was linked to a computer, and the collinear SH intensity collected by the CCD served as the feedback. At last, a searching algorithm is applied to realize the optimization. In our experiment, a stepwise sequential algorithm was used. Other commonly used searching algorithms applied in a wavefront shaping technique may include a sequential algorithm [21] and a genetic algorithm [22].

Here, a BMF single crystal was used as the weakly nonlinear scattering medium, which was grown by the temperature gradient technique [23]. The as-grown BMF crystal was cut into a cuboid with a dimension of 10 mm × 8 mm × 10 mm and then polished to an optical level. Most of the time, scattering centers in a BMF single crystal are present. The formation mechanism of scattering centers in a BMF crystal grown by Czochralski method had been studied by Zhao *et al.* [24]. It indicates that the scattering centers in a BMF single crystal are attributed to second-phase particles (crystalline precipitates), which are formed during the slow cooling process. During our BMF crystal growth process, the cooling process was set at a very low rate (0.8°C/h) to prevent cracking in the BMF crystal, and it would lead to the formation of crystalline precipitates. Illuminated with a red laser (650 nm), scattering centers can be observed in the entire crystal in the perpendicular direction [see Fig. 2(b)]. Figure 2(c) shows the transmitted beam spot when a 1064 nm laser passes through the BMF sample. Some of the fundamental beam is scattered randomly all over the free space.

Before the optimization experiment, the intensity of the generated SH in the vicinity of the BPM point was measured. The BMF crystal was placed on a rotator with a precision of 0.01°. As shown in Fig. 3, the black circular dots are the measured normalized SH intensity versus the internal incident angle. The red line is the fitting curve to experimental data with the sinc^2 function. The angle of the peak is 11.70°, which presents a good match with the theoretical BPM angle (11.69°). From the point of nonlinear coupled-wave theory, the coupled-wave equations for SHG with loss can be written as [25] follows:

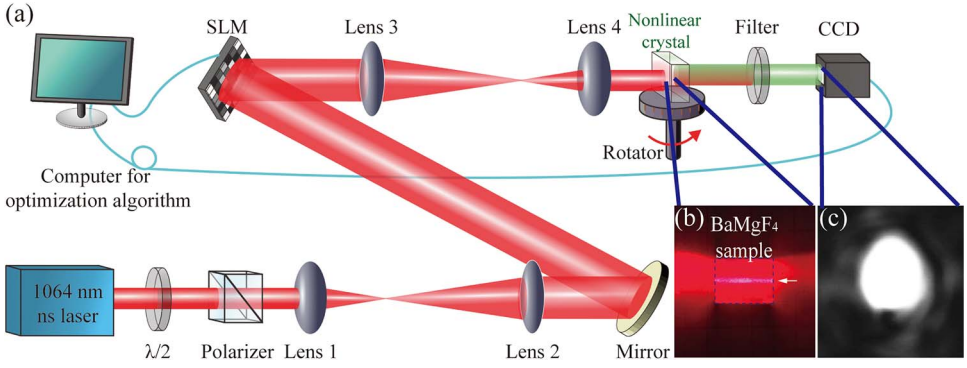

Fig. 2. (a) Schematic diagram of experimental setup for SH manipulation via wavefront shaping. $\lambda/2$, half-wave plate; $f1 = f3 = 50$ mm; $f2 = f4 = 200$ mm. (b) Weakly scattering in BMF crystal grown by temperature gradient technique. (c) The beam spot of a 1064 nm laser after the BMF sample.

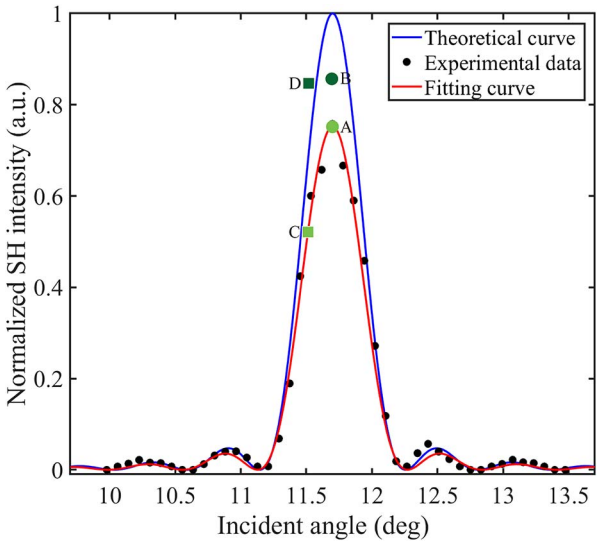

Fig. 3. Intensity of the generated SH in the vicinity of the BPM point. The black circular dots are the experimental data, and the red line is the fitting curve with the sinc^2 function. The blue line is the theoretical curve wiping off the scattering loss by numerical analysis. Points A and B are the positions corresponding to the normalized SH intensity before and after optimization under PM condition (the internal incident angle is 11.70°). Points C and D are the positions corresponding to the normalized SH intensity before and after optimization under phase-mismatching condition (the internal incident angle is 11.50°).

$$\frac{dA_\omega}{dz} = \frac{2i\omega^2 d_{\mathrm{eff}}}{k_\omega c^2} A_{2\omega} A_\omega^* e^{-i\Delta kz} - \frac{1}{2}\alpha_1 A_\omega, \tag{2}$$

$$\frac{dA_{2\omega}}{dz} = \frac{i(2\omega)^2 d_{\mathrm{eff}}}{k_{2\omega} c^2} A_\omega^2 e^{i\Delta kz} - \frac{1}{2}\alpha_2 A_{2\omega}. \tag{3}$$

Here, A_ω and $A_{2\omega}$, k_ω and $k_{2\omega}$ are the amplitudes and wave vectors of the FW and SH, respectively. d_{eff} is the effective nonlinear coefficient, and z is the propagation distance. The optical loss of the FW (1064 nm) and SH (532 nm) caused by scattering in the BMF sample is measured to be $\alpha_1 = 0.90$ dB/cm and $\alpha_2 = 0.56$ dB/cm, respectively. By numerically solving Eqs. (2) and (3), the theoretical curve after wiping off the scattering loss of the BMF crystal is displayed with the blue line. More specifically, the maximum value of normalized SH intensity at the PM point decreases to about 75.7% compared to the theoretical situation, and it is attributed to scattering loss in the BMF crystal.

Figure 4 shows the results of the optimization experiment under PM condition. The SH beam spot before optimization (Fig. 4 inset corresponding to the blue line) was nearly a circular one. Actually, our experiment is an optimization to a not bad result because the scattering in the BMF sample is relatively weak. As a result, the modulation can be considered as a perturbation to the FW. Therefore, compared to the genetic algorithm, the stepwise sequential algorithm is more suitable in our experiment, as the former one may bring in more uncertainties and randomness. The 512×512 pixels on the SLM were divided into 32×32 segments to shape the FW wavefront. During optimization, the computer changed the phase of each segment from 0 to 2π sequentially, and the phase of each

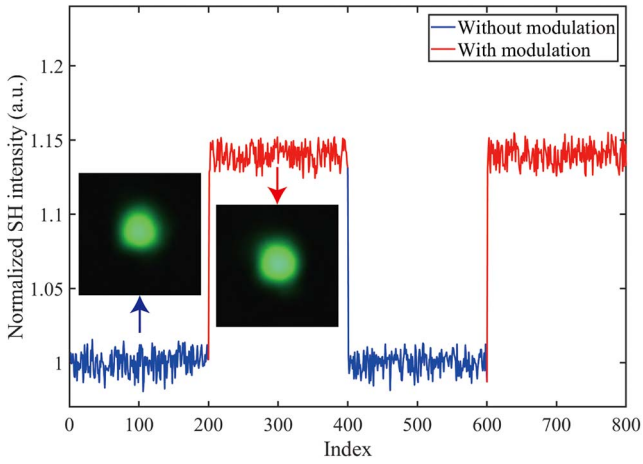

Fig. 4. Results of optimization experiment under PM condition. The blue (red) lines are normalized SH intensities without (with) modulation. Two hundred results were measured in each situation. The insets show the SH patterns recorded by the CCD before and after optimization.

segment that resulted in the highest output intensity was recorded and stored as the optimal phase. After all segments on the SLM were confirmed, the complete optimal phase masks were added on the SLM, and the modulated SH beam spot is displayed (Fig. 4 inset corresponding to the red line). It can be seen that the shape of the SH light changed only a little. The normalized SH intensity is presented. To ensure the experimental validity, 200 results were measured continuously in each situation. It is clear to see that the normalized modulated SH intensity can be enhanced by an enhancement factor of $\eta = 1.14$ when the optimal phase mask is added. After removing the optimal phase mask, the normalized SH intensity decreased back to about 1. In Fig. 3, Points A and B are the positions corresponding to the normalized SH intensity before and after optimization, respectively. Combining η with former loss value (75.7%), the overall conversion efficiency of SH intensity in the BMF crystal with scattering centers can be recovered to 86.3% by wavefront shaping. This result shows us a new method to recover the conversion efficiency in the SHG process in which the nonlinear crystals are born with various defects. Other nonlinear optical processes, such as direct third harmonic generation and three- or four-wave mixing can also be expected to show similar behavior with appropriate configurations.

We also investigated the situation when SHG is not at the PM condition. The internal incident angle was set at 11.50°. As a consequence, the collinear SH light became dimmer and the normalized SH intensity decreased to Point C (70.0% of that at Point A) in Fig. 3. Similar to the former method, the stepwise sequential algorithm was used to realize the intensity recovery of the SH light under the phase-mismatching condition. The normalized intensity increased to Point D after the optimal phase mask was added on the SLM. Figure 5 shows the experimental results and SH beam spots before and after optimization. The enhancement factor η was estimated to be 1.58, and the corresponding recovery efficiency could be determined to be 83.7%. We believe the recovery is a combination of PM correction and optimization of scattering. If we continue enlarging the phase-mismatching angle, it would deviate beyond the

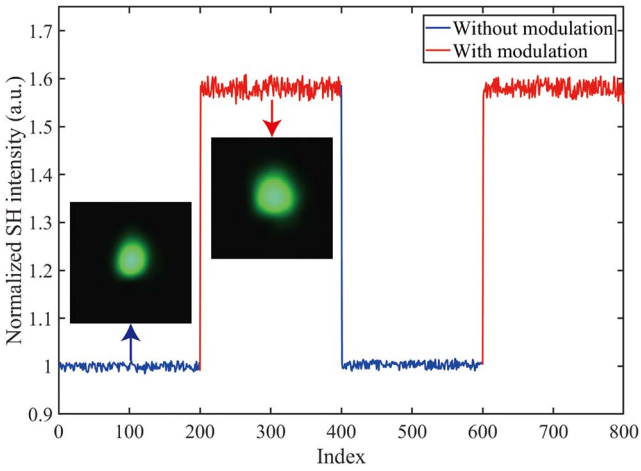

Fig. 5. Results of the optimization experiment under phase-mismatching condition. The blue (red) lines are normalized SH intensities without (with) modulation. Two hundred results were measured in each situation. The insets show SH patterns recorded by the CCD before and after optimization.

modulation limitation of the SLM and the optimization would be useless. It could be an interesting way to make conversion efficiency of BPM nonlinear processes insensitive to incident angle, refreshing the traditional understanding. In addition, it could be used as a feedback compensation for the changing temperature and other fluctuations. However, the optimization speed and recovery efficiency still limit practical applications of this method. In many cases, the higher optimization factor one expects, the more time it takes. It took about 20 min to complete our optimization process. We believe shorter time or even real-time optimization can be realized with a better software–hardware configuration and searching algorithms in the future [21,26].

In conclusion, a recovered SHG under BPM condition in a BMF single crystal with scattering centers via feedback-based wavefront shaping was demonstrated. By shaping the fundamental wavefront, the SH signal at the detected location can be modulated. The optimal phase masks of the segments on the SLM can be determined by a stepwise sequential algorithm, and the intensity of the modulated SH signal was promoted. The enhancement factor was about 1.14, and the recovery efficiency was calculated to be 86.3%. Furthermore, we experimentally realized the optimization of the SH signal under phase-mismatching condition, and the enhancement factor and corresponding recovery efficiency were determined to be 1.58% and 83.7%. This work may provide a way to recover the conversion efficiency in nonlinear wave-mixing processes with lossy media and a fine-tuning method for PM adjustment.

Funding. National Key R&D Program of China (2017YFA0303700); National Natural Science Foundation of China (NSFC) (11734011); Foundation for Development of Science and Technology of Shanghai (17JC1400400).

REFERENCES

1. R. W. Boyd, *Nonlinear Optics* (Academic, 2008).
2. S. B. Dai, N. Zong, F. Yang, S. J. Zhang, Z. M. Wang, F. F. Zhang, W. Tu, L. Q. Shang, L. J. Liu, X. Y. Wang, J. Y. Zhang, D. F. Cui, Q. J. Peng, R. K. Li, C. T. Chen, and Z. Y. Xu, Opt. Lett. **40**, 3268 (2015).
3. S. N. Zhu, Y. Y. Zhu, and N. B. Ming, Science **278**, 843 (1997).
4. H. W. Qi, Z. P. Wang, F. P. Yu, X. Sun, X. G. Xu, and X. Zhao, Opt. Lett. **41**, 5823 (2016).
5. M. Levenson, *The Principles of Nonlinear Optics* (Wiley, 1984).
6. E. G. Víllora, K. Shimamura, K. Sumiya, and H. Ishibashi, Opt. Express **17**, 12362 (2009).
7. M. Seiter, D. Keller, and M. W. Sigrist, Appl. Phys. B **67**, 351 (1998).
8. R. Akbari and A. Major, Laser Phys. **23**, 035401 (2013).
9. W. Wang, K. Y. Li, J. Wang, W. Han, F. Wang, Y. Xiang, F. Q. Li, H. T. Jia, L. Q. Wang, W. Zhong, X. M. Zhang, S. Z. Zhao, and B. Feng, Opt. Laser Technol. **43**, 683 (2011).
10. C. Y. Hu and Z. Y. Li, J. Appl. Phys. **121**, 123110 (2017).
11. V. Vaičaitis, Opt. Commun. **209**, 485 (2002).
12. H. J. Ren, X. W. Deng, Y. L. Zheng, and X. F. Chen, J. Nonlinear Opt. Phys. Mater. **20**, 459 (2012).
13. M. Baudrier-Raybaut, R. Haidar, P. Kupecek, P. Lemasson, and E. Rosencher, Nature **432**, 374 (2004).
14. C. Y. Yang, C. Lin, L. Charlotte, W. M. Su, C. Carlota, and C. S. Chuu, Sci. Rep. **6**, 26079 (2016).
15. D. B. Conkey and R. Piestun, Opt. Express **20**, 27312 (2012).
16. P. Lai, L. Wang, W. T. Jian, and L. V. Wang, Nat. Photonics **9**, 126 (2015).
17. E. Small, O. Katz, Y. Siberberg, and Y. Guan, Optica **1**, 170 (2014).
18. H. Kouta and Y. Kuwano, Appl. Opt. **38**, 1053 (1999).
19. T. L. Li, X. H. Zhao, Y. L. Zheng, and X. F. Chen, Opt. Express **23**, 23827 (2015).
20. Y. Q. Qin, C. Zhang, and Y. Y. Zhu, Phys. Rev. Lett. **100**, 063902 (2008).
21. I. M. Vellekoop and A. P. Mosk, Opt. Lett. **32**, 2309 (2007).
22. Y. Q. Qiao, Y. J. Peng, Y. L. Zheng, F. W. Ye, and X. F. Chen, Opt. Lett. **42**, 1895 (2017).
23. A. H. Wu, Z. Wang, L. B. Su, D. P. Jiang, Y. Q. Zou, J. Xu, J. J. Chen, Y. Z. Ma, X. F. Chen, and Z. G. Hu, Opt. Mater. **38**, 238 (2014).
24. C. C. Zhao, L. H. Zhang, Y. Hang, X. M. He, J. G. Yin, P. C. Hu, G. Z. Chen, M. Z. He, H. Huang, and Y. Y. Zhu, J. Cryst. Growth **316**, 158 (2011).
25. A. Yariv, *Quantum Electronics* (Wiley, 1989).
26. A. S. Hemphill, J. W. Tay, and L. V. Wang, J. Biomed. Opt. **21**, 121502 (2016).